J|A|C|S
ARTICLES
Published on Web 10/11/2006

Fungus-Mediated Biotransformation of Amorphous Silica in Rice Husk to Nanocrystalline Silica

Vipul Bansal,[†] Absar Ahmad,*[,‡] and Murali Sastry*[,†,§]

Contribution from the Nanoscience Group, Materials Chemistry Division, and Biochemical Sciences Division, National Chemical Laboratory, Pune 411 008, India

Received April 1, 2006; E-mail: a.ahmad@ncl.res.in; msastry@tatachemicals.com

Abstract: Rice husk is a cheap agro-based waste material, which harbors a substantial amount of silica in the form of amorphous hydrated silica grains. However, there have been no attempts at harnessing the enormous amount of amorphous silica present in rice husk and its room-temperature biotransformation into crystalline silica nanoparticles. In this study, we address this issue and describe how naturally deposited amorphous biosilica in rice husk can be bioleached and simultaneously biotransformed into high value crystalline silica nanoparticles. We show here that the fungus *Fusarium oxysporum* rapidly biotransforms the naturally occurring amorphous plant biosilica into crystalline silica and leach out silica extracellularly at room temperature in the form of 2−6 nm quasi-spherical, highly crystalline silica nanoparticles capped by stabilizing proteins; that the nanoparticles are released into solution is an advantage of this process with significant application and commercial potential. Calcination of the silica nanoparticles leads to loss of occluded protein and to an apparently porous structure often of cubic morphology. The room-temperature synthesis of oxide nanomaterials using microorganisms starting from potential cheap agro-industrial waste materials is an exciting possibility and could lead to an energy-conserving and economically viable green approach toward the large-scale synthesis of oxide nanomaterials.

Introduction

Silica is an extremely important inorganic material[1] and is extensively used for a wide range of commercial applications such as resins, molecular sieves, catalyst supports, fillers in polymers, as well as in biomedical applications.[2] In general, porous inorganic microstructures are of interest as low density and thermally stable particles, and also as mechanically resistant encapsulation structures. The chemical syntheses of silica-based materials are not only relatively expensive and eco-hazardous, but also often require extremes of temperature, pressure, and pH. In contrast, biosilicification by living organisms such as cyanobacteria, diatoms, sponges, and plants proceeds under mild physiological conditions and results in a diversity of complex and hierarchical biogenic silica nanostructural frameworks.[3,4]

Silicon, which is ubiquitous and quantitatively the second most prominent element in the earth crust after oxygen,[5] is released in soil by chemical and biological processes.[6,7] Plants contribute significantly to the biogeochemical cycle of silicon.[7b,c] They take up silicon from soil water in the form of water-soluble silicic acid (H_4SiO_4),[8] which is polymerized and precipitated as amorphous silica, frequently in close proximity to the transpiration conduit. After plant death, the silica returns back to the soil and the plant-decay generates humic acid, which increases the weathering activity in soils. Biocycling of silica in soil also occurs through microbial activities that involve fungi, bacteria, and actinomycetes. Thus, plants and microbes, through their intricate interplay with soil minerals, contribute appreciably to the global silicon cycle.[7,8]

In plants, silicon is accumulated mainly in the form of phytoliths,[9] which consist primarily of amorphous hydrated silica (SiO_2 with 5−15% H_2O). Examples of plants that produce phytoliths include dicots (e.g., Myrtaceae, Casuarinaceae, Proteaceae, Xanthorrhoeaceae, Mimosaceae), monocots (e.g., Cyperaceae, Gramineae, Palmae), conifers (e.g., Pinaceae, Taxodiaceae), and sphenophytes/scouring rushes (e.g., Equisetaceae).[10]

[†] Material Chemistry Division.
[‡] Biochemical Sciences Division.
[§] Current address: Tata Chemicals Ltd., Leela Business Park, Andheri-Kurla Rd., Andheri (E), Mumbai, India.

(1) Hubert, D. H. W.; Jung, M.; German, A. L. *Adv. Mater.* **2000**, *12*, 1291.
(2) (a) Iler, R. K. *The Chemistry of Silica*; John Wiley & Sons: New York, 1979. (b) Kendall, T. *Ind. Miner.* **2000**, 49. (c) Brinker, C. J.; Scherer, G. W. *Sol−Gel Science: The Physics and Chemistry of Sol−Gel Processing*; Academic Press: Boston, 1990. (d) Hench, L. L. *J. Am. Ceram. Soc.* **1991**, *74*, 1487.
(3) (a) Mann, S. *Nature* **1993**, *365*, 499. (b) Oliver, S.; Kupermann, A.; Coombs, N.; Lough, A.; Ozin, G. A. *Nature* **1995**, *378*, 47. (c) Mann, S.; Ozin, G. A. *Nature* **1996**, *382*, 313. (d) Mann, S., Webb, J., Williams, R. J. P., Eds. *Biomineralization: Chemical and Biochemical Perspectives*; VCH: Weinheim, Germany, 1998. (e) Lowenstam, H. *Science* **1981**, *211*, 1126.
(4) (a) Simpson, T. L.; Volcani, B. E. *Silicon and Siliceous Structures in Biological Systems*; Springer-Verlag: New York, 1981. (b) Levi, C.; Barton, J. L.; Guillemet, C.; Le Bras, E.; Lehuede, P. *J. Mater. Sci. Lett.* **1989**, *8*, 337. (c) Westall, F.; Boni, L.; Guerzoni, E. *Palaeontology* **1995**, *38*, 495. (d) Benning, L. G.; Phoenix, V.; Yee, N.; Konhauser, K. O. *Geochim. Cosmochim. Acta* **2004**, *68*, 743.
(5) Epstein, E. *Proc. Natl. Acad. Sci. U.S.A.* **1994**, *91*, 11.
(6) Lucas, Y.; Luizao, F. J.; Rouiller, J.; Nahon, D. *Science* **1993**, *260*, 521.
(7) (a) Treguer, P.; Nelson, D. M.; Van Bennkom, A. J.; DeMaster, D. J.; Leynaert, A.; Queguiner, B. *Science* **1995**, *268*, 375. (b) Alexandre, A.; Meunier, J. D.; Colin, F.; Koud, J. M. *Geochim. Cosmochim. Acta* **1997**, *61*, 677. (c) Derry, L. A.; Kurtz, A. C.; Ziegler, K.; Chadwick, O. A. *Nature* **2005**, *433*, 728.
(8) Barber, D. A.; Shone, G. T. *J. Exp. Bot.* **1966**, *17*, 569.
(9) Ehrenberg, C. G. *Monatsber. Koniglich Preussischen Akad. Wiss. Berlin* **1846**, 191.
(10) Hart, D. M. *Aust. J. Bot.* **1988**, *36*, 159.

The ash content of Equisetaceae and Gramineae/Poaceae may consist of up to 50−70% silica.[11] Some polyamines, carbohydrates, proteins, and glycoproteins from diatoms and sponges have been reported to be capable of polymerizing silicic acid at neutral to acidic pHs.[12] Some plant carbohydrates and proteins have also been shown to play a key role in biosilica polymerization.[13] In the biosphere, silica is accumulated predominantly in the form of amorphous silica (opal or silica gel).[4,14]

Rice (*Oryza sativa*), which is a member of the family Gramineae, typically constitutes 20−22% of its total produce in the form of rice husk, and a great deal of rice husk is presently disposed off by rice mill industry as waste. The presence of silicon as SiO_2 in rice has been well known since 1938.[15] Interestingly, the highest SiO_2 content in rice is observed in its husk, which varies from 8.7% to 12.1%, averaging close to 10.6%.[16a] However, the silica present in rice husk is in a hydrated amorphous form[14,16b] similar to that present in most of the other entities in the biosphere. While there have been some studies on the dissolution of amorphous silica present in rice hull ash (RHA) to octasilicate anions under ambient conditions,[16b] to our knowledge there have been no attempts at harnessing the enormous amount of amorphous silica present in rice husk (a cheap agro-based waste material) and its room-temperature biotransformation into crystalline silica nanoparticles. In this Article, we address this issue and describe how naturally deposited amorphous biosilica in rice husk can be bioleached and simultaneously biotransformed into high value crystalline silica nanoparticles. Our approach involves the use of *Fusarium oxysporum*, a plant pathogenic fungus, in the biotransformation of naturally occurring amorphous plant biosilica into quasi-spherical crystalline silica nanoparticles and its extracellular leaching in the aqueous environment at room temperature. The silica biotransformation is fairly rapid and occurs within 1 day of reaction of the fungal biomass with the rice husk. It is interesting to note that, despite the in vitro studies of various natural or synthetic macromolecules in this context,[17−19] only the *Fusarium oxysporum* based system was able to produce the aforesaid silica structures for the conditions studied to date. In previous studies, we have demonstrated that *Fusarium oxysporum* is an excellent microorganism for the biosynthesis of metal[20] and metal oxide[21] nanoparticles from their precursor salts. Recently, we have also shown a fungus-based bioleaching approach for the synthesis of hollow silica nanospheres from sand,[22] and the new results presented in this paper add considerably to the potential for application of this versatile fungus to nanotechnology, particularly in the development of cheap, energy-conserving, eco-friendly methods for the large-scale synthesis of nanomaterials.

Experimental Section

The rice husk used in this study was obtained from a rice milling plant at Lucknow, UP, India. The plant pathogenic fungus, *Fusarium oxysporum*, was cultured as described elsewhere.[20] After incubation, the fungal mycelia was harvested and washed thoroughly under sterile conditions. For the biotransformation of amorphous silica present in rice husk by the fungus *Fusarium oxysporum*, 100 mL of distilled water containing 10 g of rice husk was autoclaved in a 500 mL Erlenmeyer flask, and the harvested fungal biomass (20 g wet weight) was resuspended in sterile distilled water containing rice husk. The reaction between the fungal biomass and rice husk was carried out on a shaker (200 rpm) at 27 °C for a period of 24 h, and the reaction products were collected during various time intervals up to 24 h by separating the fungal mycelia and rice husk from the aqueous component by filtration. The filtrate thus obtained was treated with phenol−chloroform (1:1) and centrifuged at 6000 rpm for 10 min to remove the free extracellular fungal proteins from the aqueous solution. The purified silica nanoparticles were collected from the aqueous phase as described previously.[22] The silica nanoparticle solution was evaporated under low pressure to powder, and the powder was characterized before and after calcination at 400 °C for 2 h. In another experiment, standard amorphous silica (silica gel) was exposed to 100 mL of distilled water containing 20 g of fungal biomass for 24 h under shaking conditions, and the reaction product obtained was characterized.

For scanning electron microscopy (SEM) analysis, fragments of rice husk before and after its reaction with the fungus and after HF treatment for 24 h were fixed onto aluminum substrate holder with silver paste. SEM imaging of rice husk was performed on a Leica Stereoscan-440 instrument with energy-dispersive X-ray (EDX) attachment. Samples for transmission electron microscopy (TEM) were prepared by drop-coating films of the biotransformed silica nanoparticle powders as well as finely ground rice husk dispersed in water onto carbon-coated copper grids. Selected area electron diffraction (SAED) analysis was also carried out for these samples. TEM and SAED patterns of bioleached products were obtained on a JEOL 1200 EX instrument operated at an accelerating voltage of 120 kV. High-resolution TEM (HRTEM) images as well as EDX and SAED analysis of finely ground rice husk were obtained on a JEOL JEM-2010 UHR instrument operated at a lattice image resolution of 0.14 nm with EDX attachment. The reaction of the fungal biomass with the rice husk was monitored by Fourier transform infrared (FTIR) spectroscopy during the course of reaction up to 24 h. Samples for FTIR analysis were taken in KBr pellets and analyzed on a Perkin-Elmer Spectrum One instrument at a resolution of 2 cm^{-1}. X-ray diffraction (XRD) measurements of amorphous and crystalline silica powders and drop-coated films of the extracellularly synthesized biogenic silica at various time intervals up to 24 h of reaction and after calcination of samples at 400 °C for 2 h and deposited on glass were carried out on a Phillips PW 1830 instrument operated at a voltage of 40 kV and a current of 30 mA with Cu Kα radiation.

(11) Lanning, F. C.; Ponnaiya, B. W. X.; Crumpton, C. F. *Plant Physiol.* **1958**, *33*, 339.
(12) (a) Kroger, N.; Deutzmann, R.; Bergsdort, C.; Sumper, M. *Proc. Natl. Acad. Sci. U.S.A.* **2000**, *97*, 14133. (b) Shimizu, K.; Cha, J.; Stucky, G. D.; Morse, D. E. *Proc. Natl. Acad. Sci. U.S.A.* **1998**, *95*, 6234. (c) Sumper, M.; Kroger, N. *J. Mater. Chem.* **2004**, *14*, 2059. (d) Cha, J. N.; Shimizu, K.; Zhou, Y.; Christiansen, S. C.; Chmelka, B. F.; Stucky, G. D.; Morse, D. E. *Proc. Natl. Acad. Sci. U.S.A.* **1999**, *96*, 361.
(13) (a) Perry, C. C.; Keeling-Tucker, T. *Colloid Polym. Sci.* **2003**, *281*, 652. (b) Perry, C. C.; Keeling-Tucker, T. *J. Biol. Inorg. Chem.* **2000**, *5*, 537. (c) Perry, C. C.; Keeling-Tucker, T. *Chem. Commun.* **1998**, 2587. (d) Harrison, C. C. *Phytochemistry* **1996**, *41*, 3642.
(14) (a) Sterling, C. *Am. J. Bot.* **1967**, *54*, 840. (b) Houston, D. F. *Rice Chemistry and Technology*; American Association of Cereal Chemists: St. Paul, MN, 1972; p 301.
(15) Martin, J. L. The Desilicification of Rice Hulls and a Study of the Products Obtained. M.S. Thesis, Louisiana State University, Eunice, LA, 1938.
(16) (a) Ding, T. P.; Ma, G. R.; Shui, M. X.; Wan, D. F.; Li, R. H. *Chin. Chem. Geol.* **2005**, *218*, 41. (b) Asuncion, M. J.; Hasegawa, I.; Kampf, J. W.; Laine, R. M. *J. Mater. Chem.* **2005**, *15*, 2114.
(17) (a) Kroger, N.; Deutzmann, R.; Sumper, M. *Science* **1999**, *286*, 1129. (b) Kroger, N.; Lorenz, S.; Brunner, E.; Sumper, M. *Science* **2002**, *298*, 584.
(18) Cha, J. N.; Stucky, G. D.; Morse, D. E.; Deming, T. J. *Nature* **2002**, *403*, 289.
(19) (a) Patwardhan, S. V.; Clarson, S. J. *Silicon Chem.* **2002**, *413*, 291. (b) Patwardhan, S. V.; Clarson, S. J.; Perry, C. C. *Chem. Commun.* **2005**, 1113. (c) Mitzutani, A. J.; Nagase, H.; Fujiwara, N.; Ogoshi, H. *Chem. Soc. Jpn.* **1998**, *71*, 2017.
(20) Mukherjee, P.; Senapati, S.; Mandal, D.; Ahmad, A.; Khan, M. I.; Kumar, R.; Sastry, M. *ChemBioChem* **2002**, *3*, 461.
(21) (a) Bansal, V.; Rautaray, D.; Ahmad, A.; Sastry, M. *J. Mater. Chem.* **2004**, *14*, 3303. (b) Bansal, V.; Rautaray, D.; Bharde, A.; Ahire, K.; Sanyal, A.; Ahmad, A.; Sastry, M. *J. Mater. Chem.* **2005**, *15*, 2583. (c) Bharde, A.; Rautaray, D.; Bansal, V.; Ahmad, A.; Sarkar, I.; Yusuf, S. M.; Sanyal, M.; Sastry, M. *Small* **2006**, *2*, 135.
(22) Bansal, V.; Sanyal, A.; Rautaray, D.; Ahmad, A.; Sastry, M. *Adv. Mater.* **2005**, *17*, 889.

X-ray photoemission spectroscopy (XPS) measurements of films of biotransformed silica nanoparticles as well as finely ground rice husk before and after its reaction with the fungus, cast on to Cu strips, were carried out on a VG MicroTech ESCA 3000 instrument at a pressure better than 1×10^{-9} Torr. The general scan and C 1s, Si 2p, and O 1s core level spectra were recorded with unmonochromatized Mg Kα radiation (photon energy = 1253.6 eV) at a pass energy of 50 eV and electron takeoff angle (angle between electron emission direction and surface plane) of 60°. The overall resolution was 1 eV for the XPS measurements. The core level spectra were background corrected using the Shirley algorithm,[23] and the chemically distinct species were resolved using a nonlinear least-squares fitting procedure. The core level binding energies (BEs) were aligned with the adventitious carbon binding energy of 285 eV. Bioleaching of silica nanoparticles from rice husk was also monitored by evaluating the reduction in Si signal in EDX spectra of fungal-reacted finely ground rice husk at various time intervals.

The biomolecules occluded in the silica nanostructures were analyzed using 12% sodium dodecyl sulfate polyacrylamide gel electrophoresis (SDS-PAGE). For protein analysis, the bioleached silica particles were obtained by centrifugation at 10 000 rpm for 30 min, and the free proteins were removed by repeated washing and centrifugation. Silica nanoparticles along with the occluded proteins were treated with 3 M ammonium fluoride (NH_4F) for 48 h at 4 °C with constant stirring to dissolve silica from the proteins. Following dissolution, the protein sample was dialyzed against deionized water over 7 days, lyophilized, and analyzed using SDS-PAGE. To understand the nature of silica-bound proteins, the lyophilized protein fraction was loaded onto cationic (CM-sephadex) and anionic (DEAE-sephadex) ion exchange matrixes, respectively. The unbound fractions obtained from both of these columns were lyophilized and also checked on SDS-PAGE.

The extracellular fungal proteins obtained by inoculating 20 g of fungal biomass in sterile deionized water for 24 h was also checked for its capability to synthesize silica particles from rice husk in vitro. Briefly, 0.1 g of rice husk was suspended in 10 mL of extracellular fungal extract, and the reaction was carried out at 4 °C for 72 h. The extracellular fungal extract was concentrated by lyophilization and loaded onto CM-sephadex and DEAE-sephadex matrixes, respectively. The unbound fractions obtained from both of these columns were checked for their activity to synthesize silica particles in vitro. The reaction products formed were analyzed by FTIR, XRD, and TEM studies.

A control experiment was performed wherein the rice husk was exposed to distilled water (pH adjusted to 4.5) for 15 days without adding *Fusarium oxysporum*. The solution was further analyzed by FTIR and TEM.

Results and Discussion

To understand the morphology of amorphous silica present in the rice husk, a fragment of rice husk was imaged by SEM. Figure 1A1 and A2 shows the lower and higher magnification SEM images recorded from the upper surface of rice husk, while Figure 1B1 and B2 shows the similar images recorded from the lower surface of rice husk before its exposure to the fungus. These SEM images exhibit the presence of heterogeneously distributed silica on upper as well as lower surfaces of rice husk, which was further confirmed by EDX analysis as shown in Figure 1A3 and B3 for upper and lower surfaces, respectively. From these SEM images, one concludes that the silica present on the surface of rice husk is of micrometer dimensions with the particles being of variable morphology. The further confirmation of the presence of silica in rice husk was done by treating rice husk with hydrofluoric acid (HF), which selectively dissolutes silica particles. Figure 1C1,C2 and Figure 1D1,D2 show the SEM images obtained from upper and lower surfaces of rice husk, respectively, after HF treatment. No silica particles are visible in SEM images of Figure 1C and D that correlate well with the corresponding EDX spectra shown in Figure 1C3 and D3 from upper and lower rice husk surfaces after HF treatment, which do not show any Si signal. We observe weak fluoride signal coming from these EDX spectra due to residual fluoride ions from HF even after repeated washing of rice husk. The presence of aluminum signal is because of SEM substrate holder. The change in morphology of silica present in rice husk after its reaction with the fungus *Fusarium oxysporum* for 24 h was also studied as is shown in Figure 1E1−E5 (upper surface) and Figure 1F1,F2 (lower surface). Figure 1E2−E5 shows the higher magnification images of the various regions of upper surface of rice husk after fungal reaction as shown in Figure 1E1. We observe the formation of some pyramidical/triangular silica structures in some regions in rice husk (Figure 1E5), which give a strong Si signal in EDX (data not shown for the reason of brevity). However, the area EDX profiles from large regions of rice husk show very small Si signal as shown in Figure 1E6 and 1F3 from upper and lower surfaces of rice husk after fungal reaction. This suggests that most of the silica present in rice husk has been leached out within 24 h of its reaction with the fungus *Fusarium oxysporum*.

To quantitate the amount of silica leached out from rice husk during its course of reaction with the fungus, husk obtained after its reaction with fungus at various time intervals (0, 8, 16, 24 h) was finely ground, and EDX kinetics of ground husk was performed (Supporting Information S1, Figure A, curves 1−4, respectively). Based on the change in Si:C ratio in rice husk during the reaction, it was found by EDX analysis that interestingly 90% and 95% of silicon is leached out in 8 and 16 h of reaction, respectively, while it takes 24 h to leach out 97% of silica from rice husk. Because EDX is a semiquantitative technique, a more quantitative approach to quantitate silica bioleaching process was followed in the form of X-ray photoemission spectroscopy (XPS) analysis. Supporting Information S2 shows the Si 2p (Figure A and C) and C 1s (Figure B and D) core level XPS spectra obtained from finely ground rice husk before (Figure A and B) and after (Figure C and D) its reaction with the fungus *Fusarium oxysporum* for 24 h and their binding energies (BEs) being aligned with respect to the adventitious C 1s BE of 285 eV. The XPS signals obtained for Si 2p and C 1s were fitted using Gaussian equations, and the respective curves were integrated to obtain the area under the curves. Si:C ratios in rice husk before and after its reaction with fungus were used to quantitate the amount of silica bioleached from rice husk, and it was observed that the reaction of fungus with rice husk results in leaching out of 96% of silica from rice husk in aqueous solution within 24 h.

Figure 2A shows a representative bright field transmission electron microscopy (TEM) image recorded from a film of the extracellular product obtained by the reaction of *Fusarium oxysporum* with the rice husk for 24 h (pH of the reaction medium ~4.5). A number of particles of irregular morphology are observed in the extracellular reaction medium; the particles are small, ranging in size from 2 to 6 nm, and tend to cluster. Selected area electron diffraction (SAED) analysis of the particle assemblies (inset, Figure 2A) clearly indicates that the particles

(23) Shirley, D. A. *Phys. Rev. B* **1972**, *5*, 4709.

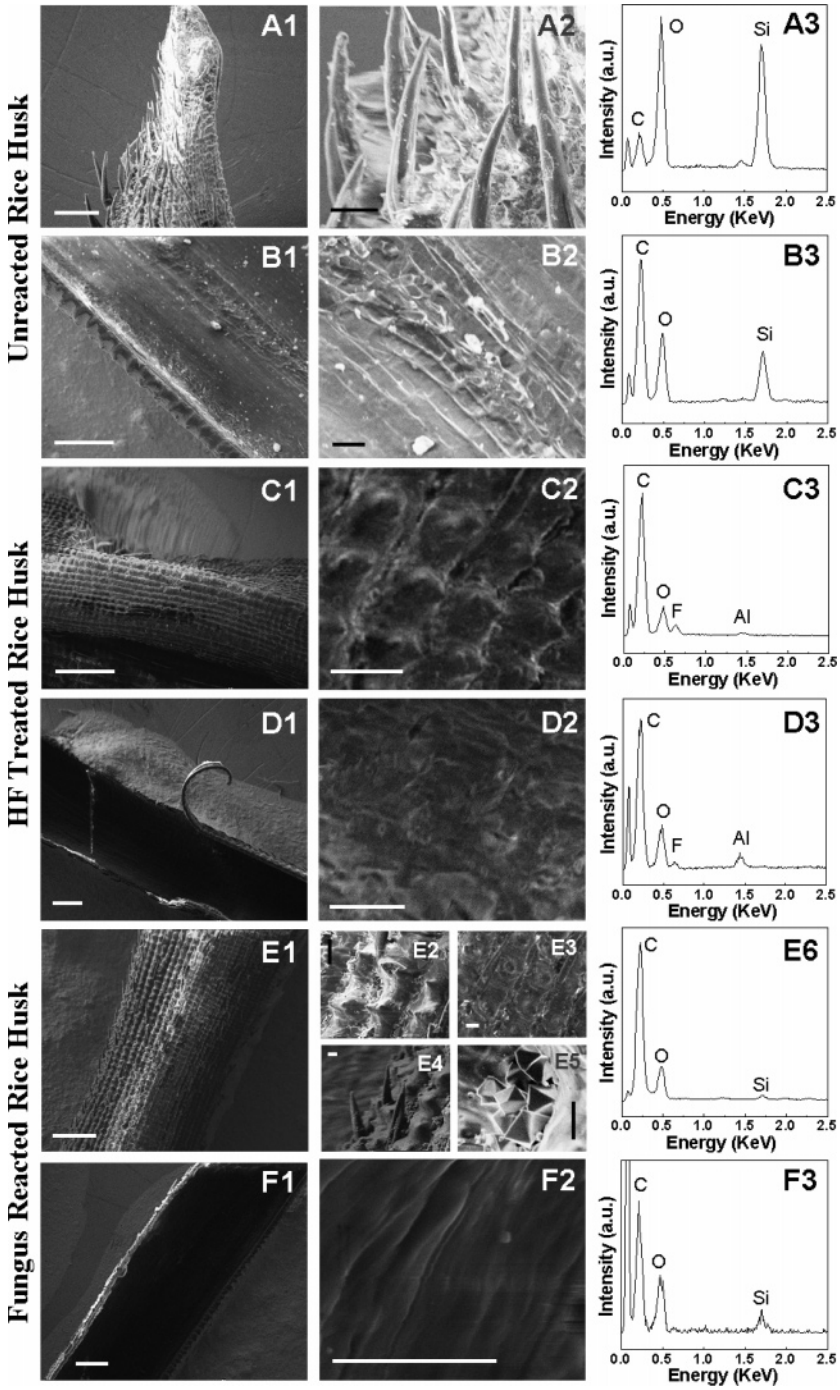

Figure 1. SEM micrographs (columns 1 and 2) and corresponding EDX spectra (column 3) of upper (panels A, C, and E) and lower (panels B, D, and F) surfaces of rice husk before (A1−A3 and B1−B3) and after (E1−E6 and F1−F6) its reaction with the fungus *Fusarium oxysporum* and after its treatment with hydrofluoric acid (C1−C3 and D1−D3). Columns 1 and 2 show the low and high magnification SEM images of a single rice husk flake, while column 3 shows the EDX spectra from their respective high magnification field views shown in column 2. (See text for details.) Scale bars in the images shown in the first column (A1−FI) correspond to 500 μm, while those in the second column correspond to 50 μm (A2−F2).

are crystalline. The diffraction spots in the SAED pattern could be indexed on the basis of the quartz polymorph of silica.[24] Figure 2B shows a representative bright field TEM image recorded from silica nanoparticles after removal of free proteins in solution by phenol−chloroform treatment. Removal of unbound proteins clearly enhances the quality of the TEM image of the nanoparticles (Figure 2B). The particles embedded in the biomolecular matrix are fairly regular in shape and depict an overall quasi-spherical morphology (Figure 2B).

To understand the mechanism of leaching out of silica from rice husk in the form of silica nanoparticles, a time-dependent FTIR analysis of particles from the fungus−rice husk reaction medium taken in KBr pellets was carried out after 4, 8, 12, 16, 20, and 24 h of reaction (Figure 3A, curves 2−7, respectively). Curve 2 in Figure 3A corresponds to the FTIR spectra of bio-leached product recorded at early stage of reaction (after 4 h),

(24) The XRD patterns were indexed with reference to the crystal structures from the PCPDF charts: silica (PCPDF card nos. 46-1045 and 40-1498).

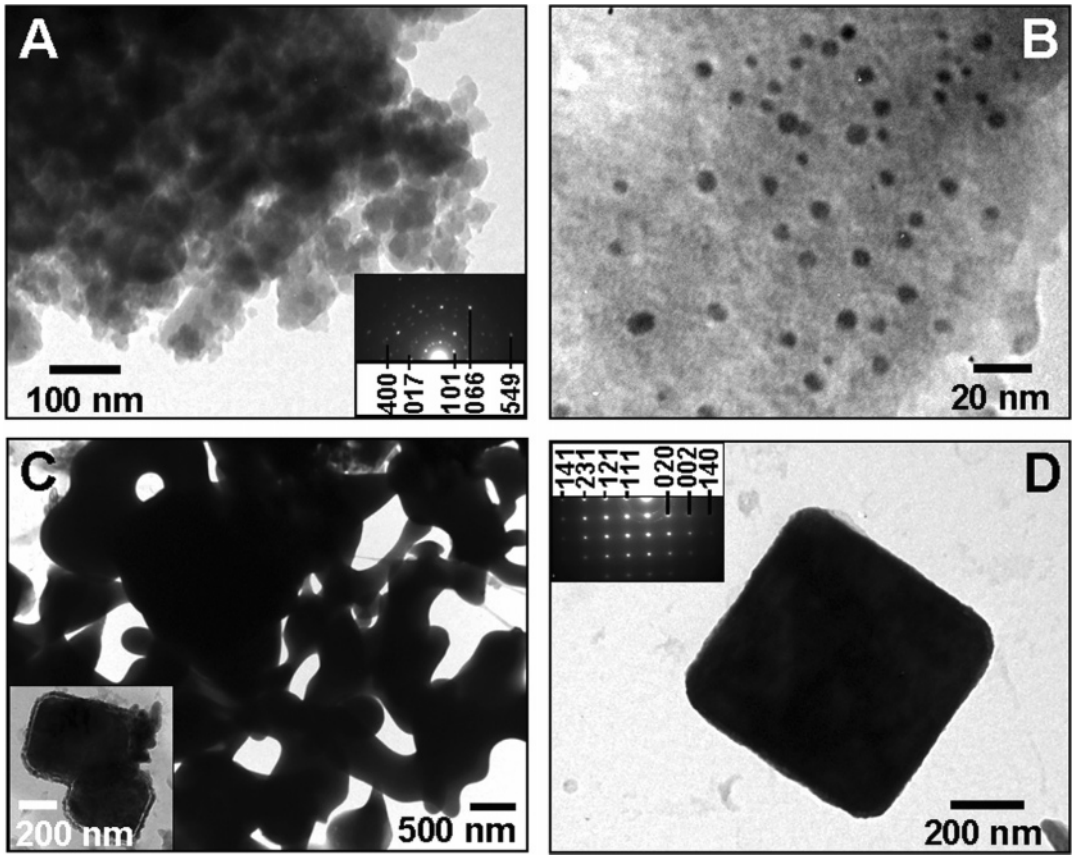

Figure 2. TEM micrographs at different magnifications of silica nanoparticles synthesized by the exposure of rice husk to the fungus *Fusarium oxysporum* before (A and B; text for details) and after calcination at 400 °C for 2 h (C and D). The inset in (C) corresponds to a high magnification image of silica particles shown in the main figure. The insets in (A) and (D) are SAED patterns recorded from representative silica nanoparticles in the corresponding images.

wherein we observe a shoulder around 900 cm^{-1}. We also observe a concomitant reduction in the peak at ca. 900 cm^{-1} as the reaction proceeds from 4 to 24 h (Figure 3A, curves 2−7, respectively). Another interesting feature is the presence of a rather broad peak at ca. 1050−1250 cm^{-1} up to 8 h of reaction (Figure 3A, curves 2 and 3) with a maximum at 1070 cm^{-1}. This peak can be assigned to the Si−O−Si antisymmetric stretching mode (TO_3 mode) present in the leached out product.[25] The TO_3 mode is generally accompanied by a shoulder toward higher frequency side. Interestingly, during the initial course of reaction, we do not observe any such shoulder (curves 2 and 3); however, after 8 h of reaction (curves 4−7), the broad feature at ca. 1050−1250 cm^{-1} starts resolving into smaller components, and we observe a shoulder developing at around 1150 cm^{-1} that becomes very clear after 24 h of reaction (curve 7). To understand the gradual loss in intensity of the shoulder toward lower wavenumber (∼900 cm^{-1}) and a gradual growth of the peak toward higher wavenumbers (∼1150 cm^{-1}), FTIR analysis of standard silica samples, amorphous silica (silica gel) and crystalline silica (quartz), was also performed (Supporting Information S3A). Interestingly, the standard amorphous silica sample shows FTIR spectra similar to that from the reaction product obtained during beginning of reaction (a broad peak around 1100 cm^{-1} with a shoulder at around 900 cm^{-1}) (compare curve 2, Figure 3A and Supporting Information S3A). However, standard crystalline quartz sample shows FTIR spectra

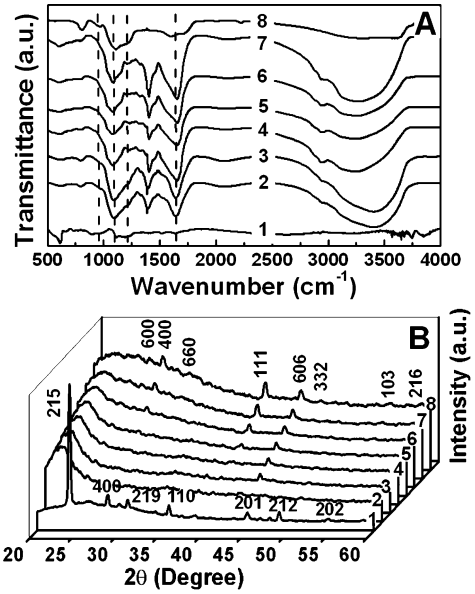

Figure 3. (A) FTIR spectra recorded from the filtrate containing silica particles synthesized by exposing rice husk to the fungus *Fusarium oxysporum* for 24 h (curves 2−7), from silica nanoparticles calcined at 400 °C for 2 h (curve 8), and from the filtrate obtained by exposing rice husk to water of pH 4.5 for 15 days (curve 1). Curves 2−7 correspond to silica particles formed at 4, 8, 12, 16, 20, and 24 h, respectively. (B) XRD patterns recorded from silica particles synthesized by the exposure of rice husk to the fungus *Fusarium oxysporum* before (curves 3−8) and after calcination at 400 °C for 2 h (curve 1). Curve 2 corresponds to XRD pattern obtained from rice husk, while curves 3−8 correspond to silica particles formed at 4, 8, 12, 16, 20, and 24 h, respectively.

(25) Innocenzi, P.; Falcaro, P.; Grosso, D.; Babonneau, F. *J. Phys. Chem. B* **2003**, *107*, 4711.

similar to that obtained from the reaction product obtained toward the end point of reaction (a prominent peak around 1100 cm^{-1} with a shoulder at around 1150 cm^{-1} and shoulder around 900 cm^{-1} missing) (compare curve 7, Figure 3A and Supporting Information S3A). These features in the FTIR spectra of bioleached silica particles indicate the room-temperature transformation of amorphous silica into crystalline form, as the reaction proceeds. At the initial stages of reaction (4 h), it is most likely that the hydrolyzing enzyme(s) secreted by the fungus *Fusarium oxysporum* act on silica present in rice husk and bioleach amorphous silica in the aqueous solution, thus revealing a shoulder toward lower wavenumber (900 cm^{-1}) at the initial stages of reaction (Figure 3A, curves 2 and 3). The disappearance of lower wavenumber shoulder at the later stages of reaction (Figure 3A, curves 4−7) with concomitant sharpening of the Si−O−Si peak (1100 cm^{-1}) and intensification in shoulder toward higher wavenumber (1150 cm^{-1}) indicate that some biomolecules/proteins might form a complex with amorphous silica bioleached from rice husk and crystallize it to form crystalline silica nanoparticles. This is in good agreement with TEM results that revealed a high concentration of bioleached silica nanoparticles embedded in protein matrix (Figure 2A and B). The presence of a broad and intense amide band between 1500 and 1700 cm^{-1} further confirms the entrapment of proteins released by the fungus in the quasi-spherical silica particles (Figure 3A, curves 2−7). When the silica particles are calcined at 400 °C for 2 h, the amide signatures as well as the signatures from organic molecules around ca. 1400 cm^{-1} in FTIR spectra fade away, indicating the removal of most of the biomolecules during calcination (Figure 3A, curve 8).

The crystallization progression of silica particles was studied by X-ray diffraction (XRD) analysis of the bioleached product formed in the fungus−rice husk reaction medium at 4, 8, 12, 16, 20, and 24 h of reaction (Figure 3B, curves 3−8, respectively). It is evident from curves 3−8 in Figure 3B that as the fungus−rice husk reaction proceeds from 0 to 24 h, the crystallinity of silica particles increases, and, after 24 h of reaction (Figure 3B, curve 8), the silica nanoparticles show well-defined Bragg reflections characteristics of quartz polymorph of crystalline silica.[24] The XRD measurements of standard amorphous silica (silica gel) as well as crystalline silica (quartz) powders were also performed for the sake of comparison (Supporting Information S3B).

To comprehend the effect of fungus *Fusarium oxysporum* on commercially available standard amorphous silica, silica gel was exposed to the fungus, and reaction product obtained after 24 h of reaction was analyzed by FTIR and XRD (Supporting Information S4). FTIR analysis (Supporting Information S4A) of silica gel shows that the previously discussed smaller peak at ca. 950 cm^{-1} is clearly missing after exposure of silica gel to the fungus *Fusarium oxysporum*. In addition, there is development of a shoulder toward the high wavenumber side of the 1100 cm^{-1} peak. These results are similar to that observed in the case of rice husk when exposed to the fungus, which suggests that the fungus is capable of transforming amorphous silica gel into crystalline silica. The proof of crystallinity is more evident by XRD analysis of silica gel (Supporting Information S4B), wherein amorphous silica gels do not show any Bragg reflections, while after exposure to the fungus, we observe the development of a few diffraction planes in the form of Bragg reflections, which correspond to the quartz polymorph of silica. Thus, the FTIR and XRD results clearly indicate that specific biomolecules/proteins released by the fungus first leach out the amorphous silica from the rice husk and then biotransform this amorphous silica into crystalline silica particles.

It is worth mentioning that the XRD analysis of the rice husk used in this study did not show the presence of crystalline silica (Figure 3B, curve 2). Moreover, to validate the absence of crystalline silica in rice husk, SAED of finely ground rice husk was also attempted along with EDX measurement (Supporting Information S1B). We could neither observe any lattice planes in HRTEM image of silica in rice husk, nor could we obtain any electron diffraction from the same (inset, Supporting Information S1B). However, at the same time, we could record the Si signal arising from silica particles in rice husk (Supporting Information S1B). This abolishes the possibility of the presence of any crystalline silica in the starting material (rice husk). To preclude the possibility of leaching out of silica due to the acidic nature of the reaction medium, a control experiment was performed wherein the rice husk was kept in distilled water maintained at an acidic pH of 4.5 for 15 days and then the filtrate was characterized by FTIR spectroscopy and TEM. We observed that characteristic Si−O−Si vibrational modes[25] of silica as well as signatures from silicic acid (Si−OH vibrational modes)[26] were clearly missing in the control rice husk sample not exposed to the fungus (Figure 3A, curve 1). In addition, the amide signatures arising from the extracellular fungal proteins were also missing from the fungus-deficient control sample (Figure 3A, curve 1). No particles could be detected in the TEM micrographs of drop cast films from the control experiment. The control experiment and the TEM, FTIR, and XRD results of the fungus−rice husk reaction medium clearly show that amorphous silica present in the rice husk is biotransformed by the fungus and is leached out from the rice husk in the form of crystalline silica nanoparticles.

A chemical analysis of the biotransformed crystalline silica nanoparticles was performed by EDX and XPS analysis. Curve 5 in the Supporting Information S1A shows the EDX spectrum from as-synthesized silica particles. Curve 5a in the inset of the main figure shows the higher magnification region of the curve shown in the main figure. The presence of the C signal along with Si and O signal suggests the presence of biomolecules occluded in the silica nanostructures. A detailed chemical analysis of biotransformed silica particles was also performed by XPS, which is known to be a highly surface sensitive technique. Figure 4 shows the Si 2p and O 1s core level XPS spectra of the bioleached product. Figure 4A shows the Si 2p spectrum, which could be resolved into two spin−orbit pairs (spin−orbit splitting ~0.6 eV) with $2p_{3/2}$ BEs of 100.5 eV (curve 1 in Figure 4A) and 103.3 eV (curve 2 in Figure 4A), respectively. The high BE component at 103.3 eV agrees excellently with values reported for SiO_2,[27] while the low BE component at 100.5 eV[28] can be assigned collectively to the signals arising from suboxidation states of silicon. It is known that silicon suboxides (and hydroxides) show Si $2p_{3/2}$ binding energies in the interval 100.5−102.5 eV;[28] attempts to resolve these suboxides failed due to small BE shifts between them.

(26) Silverstein, R. M. *Spectrometric Identification of Organic Compounds*, 2nd ed.; John Wiley & Sons: New York, 1967; p 102.
(27) Oya, A.; Beguin, F.; Fujita K.; Benoit, R. *J. Mater. Sci.* **1996**, *31*, 4609.
(28) Graham, M. J. *Corros. Sci.* **1995**, *37*, 1377.

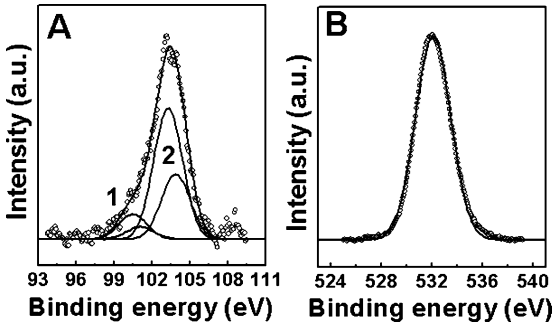

Figure 4. Si 2p (A) and O 1s (B) core level spectra recorded from biologically synthesized silica nanoparticles from rice husk cast onto a Cu substrate (see text for details). The chemically resolved components are shown as solid lines in the figure and are discussed in the text.

From the peak intensities of curve 2 (SiO_2) and curve 1 (silicon suboxides), it is observed that the amount of suboxides formed is extremely small, indicating that most of the bioleached silica is in the form of SiO_2 nanoparticles. In addition to the Si 2p spectrum, the O 1s signal was also recorded in the sample (Figure 4B) and shows a single relatively broad peak with a BE of 532.1 eV. Oxygen in the Si−O−Si environment has been reported to possess a O 1s BE of 532.3 eV,[29] while oxygen in $Si(OH)_4$ has an O 1s BE of 531.9 eV.[30] We believe that both of these components contribute to the XPS spectra shown in Figure 4B.

The FTIR results show the presence of proteins in the silica nanoparticles prepared by reaction of *Fusarium oxysporum* with rice husk. To decompose the proteins that are intercalated/incarcerated into the silica structures, calcination of the powder obtained (by drying the filtrate) was carried out at 400 °C for 2 h. The calcined silica sample was chemically analyzed by EDX (curves 6 and 6a, Supporting Information S1A). EDX results suggest that most of the carbon is removed from the silica matrix after calcination at 400 °C for 2 h (compare curve 6a (calcined sample) with curve 5a (uncalcined sample)). The calcined silica nanoparticle powder was then cast onto grids and analyzed by TEM (Figure 2C and D). It is observed that the breakdown of entrapped biomolecules by calcination leads to sintering of the silica nanoparticles and the formation of large, apparently porous silica structures of flat morphology (Figure 2C and D). Higher magnification images of these particles indicate that these structures might be porous and encompass several silica particles of nanometric dimensions (inset, Figure 2C). Apart from the entangled network of these flat structures (Figure 2C), we also notice a large number of cubic (Figure 2D) and cuboid (inset, Figure 2C) silica structures in the calcined sample. It thus appears that the proteins occluded in the silica mosaic structures (Figure 2A and B) leave behind a porous network after their degradation during calcination (Figure 2C and D). The SAED pattern recorded from these silica structures (inset, Figure 2D) clearly indicates the highly crystalline nature of the silica particles. In addition, the crystallinity of these silica nanostructures was further confirmed by XRD (Figure 3B, curve 1). The XRD analysis of the calcined powder shows well-defined Bragg reflections characteristic of quartz polymorph of silica nanoparticles.[24] It is obvious that calcination and the consequent degradation of proteins from the silica matrix results in increased crystallinity (Figure 3B, curve 2) of the silica particles when compared to the as-synthesized silica nanoparticles (Figure 3B, curve 1).

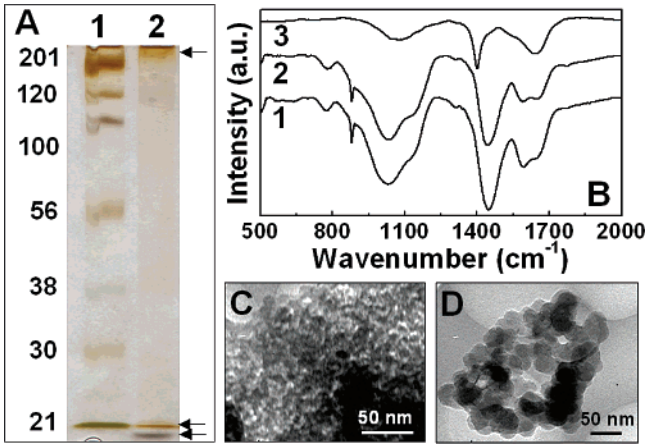

Figure 5. (A) 12% SDS-PAGE data showing the silver stained fungal proteins bound onto the surface of silica particles bioleached from rice husk using the fungus *Fusarium oxysporum* along with the standard protein molecular weight markers with their molecular weights indicated in kDa. Lane 1 corresponds to standard protein molecular weight markers (myosin, 201 kDa; β-galactosidase, 120 kDa; bovine serum albumin, 100 kDa; ovalbumin, 56 kDa; carbonic anhydrase, 38 kDa; soybean trypsin inhibitor, 30 kDa; and lysozyme, 21 kDa). Lane 2 corresponds to the proteins bound to silica particles, obtained by mild dissolution of silica particles by ammonium fluoride treatment. (B) FTIR spectra of the reaction products from in vitro exposure of rice husk to total extracellular proteins (curve 1), cationic extracellular proteins (curve 2), and anionic extracellular proteins (curve 3) of the fungus *F. oxysporum.* (C and D) TEM images of silica particles formed under in vitro conditions using total extracellular proteins (C) and cationic extracellular proteins (D) from the fungus *F. oxysporum.*

To identify the biomolecules bound to silica nanoparticles, the purified silica particles were treated with ammonium fluoride, which selectively dissolves silica without causing significant harm to nonglycosylated proteins. For the proteins occluded within the silica matrix, when analyzed using 12% SDS-PAGE, two low molecular weight proteins of around 15−20 kDa and a very high molecular weight protein of more than 200 kDa were observed (Figure 5A). It is likely that the low molecular weight proteins might be acting as hydrolyzing/capping proteins and that the high molecular weight proteins could be acting as a template for nanosilica synthesis. To understand the nature of these silica-bound proteins, the proteins obtained by ammonium fluoride treatment were initially loaded on DEAE-sephadex and CM-sephadex ion-exchange matrixes. The unbound cationic and anionic protein fractions obtained from DEAE-sephadex and CM-sephadex columns, respectively, were loaded onto SDS-PAGE. Interestingly, on SDS-PAGE analysis, we observed that all three protein bands were cationic and there was no protein present in the anionic fraction (data not shown for the reasons of brevity). This indicates that the proteins involved in the biosilicification process are cationic in nature.

To appreciate the role of extracellular fungal proteins in the silica bioleaching and biotransformation process, the in vitro synthesis of silica particles from total extracellular fungal proteins as well as from cationic and anionic fractions obtained was also monitored using FTIR, XRD, and TEM analysis (Figure 5B−D). FTIR spectra of silica particles synthesized using total extracellular fungal proteins (curve 1, Figure 5B) and cationic extracellular protein fraction (curve 2, Figure 5B)

(29) Barr, T. L. *J. Phys. Chem.* **1978**, *82*, 1801.
(30) Mink, G.; Varsanyi, G.; Bertoti, I.; Grabis, J.; Vaivads, J.; Millers, T.; Szekely, T. *Surf. Interface Anal.* **1988**, *12*, 527.

clearly indicate the bioleaching of silica from rice husk, as is evident from a peak centered about 1050 cm^{-1}. Figure 5C and D shows the corresponding TEM images of silica particles synthesized using total extracellular protein fraction (Figure 5C) and cationic protein fraction (Figure 5D), respectively. It is worth mentioning that in the reaction of rice husk with anionic fraction, although depicted as a low intensity broad signature close to 1100 cm^{-1}, no particles could be observed in TEM measurements. XRD measurements of the above three in vitro reaction products were also performed; however, XRD analysis of these samples revealed the absence of any crystallinity in the material. The absence of crystallinity in silica nanoparticles synthesized under in vitro conditions suggests that metabolic energy considerations in silica biotransformation process cannot be neglected and, in addition to extracellular fungal proteins, fungal metabolism might also be playing some role in imparting crystallinity to amorphous silica. The understanding of the role of fungal mechanism would definitely be an issue of great interest in future investigations.

In conclusion, we have demonstrated that the fungus *Fusarium oxysporum* may be used to biotransform amorphous silica present in rice husk into highly crystalline silica nanoparticles. The silica synthesized is in the form of nanoparticles capped by stabilizing proteins in the size range 2−6 nm; that the nanoparticles are released into solution is an advantage of this process with significant application and commercial potential. Calcination of the silica nanoparticles leads to loss of occluded protein and apparently leads to a porous structure often of cubic morphology. The amorphous silica particles can also be bioleached from rice husk under in vitro conditions using cationic extracellular proteins; however, these proteins alone do not lead to biotransformation of amorphous silica into silica nanocrystallites. The room-temperature synthesis of oxide nanomaterials using microorganisms starting from potential cheap agro-industrial waste materials is an exciting possibility and could lead to an energy-conserving and economically viable green approach toward the large-scale synthesis of oxide nanomaterials.

Acknowledgment. V. B. thanks the Council of Scientific and Industrial Research (CSIR), Government of India, for financial support. We thank Dr. P. V. Satyam for use of HRTEM facilities at the Institute of Physics, Bhubaneshwar, India. We acknowledge the Department of Science and Technology, Government of India, for setting up a unit on Nanoscience and Technology (DST-UNANST) at NCL, Pune, India.

Supporting Information Available: (S1) EDX spectra recorded from rice husk during the course of its reaction with the fungus, as well as spectra from as-synthesized and calcined bioleached product; HRTEM image of silica present in rice husk and SAED from particles. (S2) Si 2p and O 1s core level XPS spectra recorded from rice husk before and after its reaction with the fungus *Fusarium oxysporum*. (S3) FTIR and XRD spectra from standard amorphous silica (silica gel) and crystalline silica (quartz). (S4) FTIR and XRD spectra obtained during exposure of standard amorphous silica (silica gel) to the fungus *Fusarium oxysporum*. This material is available free of charge via the Internet at http://pubs.acs.org.

JA062113+